Quantitative Accuracy of CT Protocols for Cross-sectional and Longitudinal Assessment of COPD: A Virtual Imaging Study

Mridul Bhattarai[1], Daniel W. Shin[2], Fong Chi Ho[1], Saman Sotoudeh-Paima[1], Ilmar Hein[2], Steven Ross[2], Naruomi Akino[2], Kirsten L. Boedeker[2], Ehsan Samei[1], Ehsan Abadi[1]

1. Center for Virtual Imaging Trials, Department of Radiology, Duke University, Durham, USA
2. Canon Medical Systems, Otawara, Japan

Abstract

Chronic obstructive pulmonary disease (COPD), encompassing chronic bronchitis and emphysema, requires precise quantification through CT imaging to accurately assess disease severity and progression. However, inconsistencies in imaging protocols often lead to unreliable measurements. This study aims to optimize CT acquisition and reconstruction protocols for cross-sectional and longitudinal CT measurements of COPD using a virtual (*in-silico*) imaging framework. We developed human models at various stages of emphysema and bronchitis, informed by the COPDGene cohort. The specifications of a clinical CT scanner (Aquilion ONE Prism, Canon Medical Systems) were integrated into a CT simulator. This simulation framework was validated against experimental data. The analysis focused on the impact of tube current and kernel sharpness on two COPD biomarkers: LAA-950 (percentage of lung voxels with attenuation less than -950 HU) and Pi10 (the square root of the wall area around an airway with an internal perimeter of 10 mm) and mean absolute error (MAE; a voxel-wise error metric for emphysema density measurements). The increase in dose level showed minimal impact on the Pi10 measurements, but affected the LAA-950, with a reduction in variability observed at higher dose levels. Increasing kernel sharpness introduced variability in the LAA-950 and Pi10 measurements and higher MAE with sharper kernels. Longitudinal analysis demonstrated that kernel sharpness contributed more to variability in the COPD biomarker measurements over time compared to dose level. Similarly, cross-sectional assessments showed that an increase in MAE, while a decrease in Pi10 measurement error with sharper kernels. The study underlines the need for standardized task-specific imaging protocols to enhance the reliability and accuracy of COPD assessments, thus improving diagnostic precision and patient assessments.

Keywords

Chronic obstructive pulmonary disease, emphysema, chronic bronchitis, virtual imaging framework, XCAT

Medical Imaging 2025: Physics of Medical Imaging, edited by John M. Sabol, Ke Li, Shiva Abbaszadeh, Proc. of SPIE Vol. 13405, 134054B · © 2025 SPIE
1605-7422 · doi: 10.1117/12.3046945

Introduction

Chronic obstructive pulmonary disease (COPD) is a major cause of death in the US, characterized by chronic bronchitis and emphysema. Bronchitis is the inflammation of the bronchi, leading to airway obstruction. Emphysema is the destruction of the alveoli (air sacs in the lungs), leading to reduced surface area for gas exchange. Both conditions lead to airflow obstruction and respiratory complications (1, 2).

Quantitative CT has been used to image the pathological changes in the lungs and measure the biomarkers to characterize the severity of bronchitis and emphysema. Accurate quantification of these biomarkers is essential for proper diagnosis, treatment, and monitoring of COPD progression. However, the absence of standardized protocols for CT image acquisition and reconstruction settings may lead to inconsistent and inaccurate quantification. The purpose of this study was to systematically evaluate and optimize CT image acquisition and reconstruction protocols to enhance the accuracy of emphysema and chronic bronchitis quantification, both cross-sectionally and longitudinally. This was achieved using a virtual (also called *in-silico*) imaging framework (3) as it allows the imaging of same patients at different stages of the disease progression with different acquisition techniques, which may not be possible or ethically feasible in human clinical trials. In addition, the availability of ground-truth information allows the evaluation of image degradation caused by different imaging techniques, which is not possible with human clinical trials. The utilization of virtual imaging frameworks acquainted with realistic scanner simulators and digital human models have been utilized across multiple studies for task-specific evaluation and optimization of different imaging technologies and techniques (1, 2, 4-6).

In this study, we incorporated the specifications of a clinical scanner into a CT simulator, validated the framework against experimental data, and scanned the virtual patients amended with variable severity of bronchitis and emphysema conditions as per the stage of the disease condition. The goal is to improve patient outcomes by optimizing imaging protocols for precise, consistent, and reliable measurement of the COPD biomarkers.

Methods

The framework of this study is illustrated in **Figure 1**.

Figure 1. The framework of this study, involving virtual XCAT patients and a virtual clinical scanner.

Human modeling

Anthropomorphic computational XCAT phantoms (7) were created with varied severity of emphysema and bronchitis (1, 2, 5). The progression of these pathologies was modeled based on clinical data obtained from the COPDGene dataset (8) across three different time points, named as stage 1, 2, and 3 in this study,

CT scanner modeling

The specifications of a clinical CT scanner (Aquilion ONE Prism, Canon Medical Systems) were incorporated into a CT simulator (DukeSim) (9), designed to generate scanner-specific projection images of voxelized computational phantoms. The specifications included source spectrum, source profiles across fan and cone angles modeling bowtie filter and anode heel effect, focal spot size, source-to-detector and source-to-isocenter distances, number of rows and channels, and size of detector pixel.

The simulator was validated through a comparative analysis of task-generic image quality metrics – modulation transfer function (MTF) and noise power spectrum (NPS) (10) between real and simulated images. Spatial frequencies at 50% and 20% of the MTF, namely f_{50} and f_{20}, respectively, were measured from simulated ACR phantom (11) images and compared against their values obtained from the CT scanner manual. Noise magnitude and normalized NPS were measured from the real and simulated CT images of a 32-cm water phantom.

COPD assessment

The virtual patients were scanned using DukeSim with a small focal spot, 120 kV tube voltage, three tube currents (160, 320, 560 mA), pitch of 0.813, and gantry rotation speed of 0.5 second per rotation. The resulting CT sinograms were reconstructed using vendor's reconstruction software with FBP reconstruction algorithm, three kernels – FC08 (body sharp with BHC on), FC18 (body sharp with BHC off), and FC52 (lung kernel), slice thickness of 3 mm, FOV of 500 mm, and matrix size of 512×512.

Two clinically relevant biomarkers were analyzed for the quantification of emphysema and bronchitis: LAA-950, defined as the percentage of lung voxels with attenuation less than -950 HU, and Pi10, defined as the square root of the wall area around an airway with an internal perimeter of 10 mm. Additionally, mean absolute error (MAE) was measured as the voxel-wise mean absolute difference between CT and corresponding ground-truth images. In this study, the ground-truth was derived from the XCAT phantom image in HU, calculated at the effective energy of the source spectrum. These LAA-950, Pi10, and MAE measurements enabled both cross-sectional accuracy evaluation and longitudinal consistency assessment of COPD quantification.

Results

Figure 2 shows the validation results comparing measurements between the real and experimental images. The differences in the f_{50} of the MTF were 0.073 mm^{-1} and 0.384 mm^{-1} for the FC08 and FC52 kernels, respectively, while the differences in the f_{20} of the MTF were 0.094 mm^{-1} and 0.408 mm^{-1}. The differences in the average frequency of the NPS, calculated from normalized NPS plots, were 0.010 mm^{-1} for FC08 and 0.020 mm^{-1} for FC52. The differences in noise magnitude were 3.7 HU $\pm$ 1.1 for FC08 and 57.3 HU $\pm$ 8.0 for FC52.

Figure 3 illustrates the ground-truth and corresponding CT images of voxelized COPD human models across three stages, with emphysema and airway walls highlighted. The zoomed-in view at stage-1 emphasizes the bronchial wall region.

When the tube current increased from 160 to 560 mA, the LAA-950 for stages 1, 2, and 3 changed up to -1.47% $\pm$ 2.45, -1.07% $\pm$ 1.54, and -1.50% $\pm$ 2.45, respectively. When the kernel sharpness increased from FC08 to FC52, the LAA-950 values changed up to 6.10% $\pm$ 2.13, 6.00% $\pm$ 1.30, and 5.41% $\pm$ 2.10 for stages 1, 2, and 3. This, along with **Figure 4**, indicates that changes in kernel sharpness led to greater variability and inconsistency in the LAA-950 measurements.

As the tube current increased from 160 to 560 mA, Pi10 changed up to 0.55 mm $\pm$ 0.62, 0.13 mm $\pm$ 0.20, and 0.11 mm $\pm$ 0.36, for the stage 1, 2, and 3, respectively. When the kernel changed from FC08 to FC52, Pi10 changed up to -1.130 mm $\pm$ 0.590, -0.496 mm $\pm$ 0.326, and -0.698 mm $\pm$ 0.323 for stages 1, 2, and 3, respectively.

From 160 to 560 mA, MAE for stage 1, 2, and 3 changed up to -4.0 HU $\pm$ 6.0, -4.1 HU $\pm$ 6.1, -3.8 HU $\pm$ 6.6, respectively. From FC08 to FC52, MAE changed up to 16.2 HU $\pm$ 5.2, 16.6 HU $\pm$ 5.4, and 15.0 HU $\pm$ 5.8 for stage 1, 2, and 3. As the sharpness increased, MAE increased, indicating higher error in emphysema density measurements (**Figure 5**).

Figure 6 shows cross-sectional assessment of MAE and Pi10 measurements' accuracy. The error in emphysema density measurement, represented by MAE, increased by 12.3 HU from FC08 to FC52 kernel. In contrast, the error in Pi10 measurement decreased by 0.42 mm from FC08 to FC52. For both MAE and Pi10, tube current did not seem to affect the accuracy of emphysema density and Pi10 measurements.

Figure 2. Image quality metrics: f_{50} and f_{20} of MTF (left), normalized NPS (middle), and noise magnitude (right) measured from real and simulated CT images of ACR and 32-cm-water phantoms.

Figure 3. Qualitative analysis. Ground-truth COPD XCAT (top row) and corresponding CT images (bottom row) acquired with 560 mA, FBP algorithm, and FC18 kernel across three stages of disease progression (columns). The zoomed-in view emphasizes the bronchial wall region.

Figure 4. Quantitative longitudinal analysis: LAA-950 in % (top) and Pi10 in mm (bottom) differences between two stages: Stage2 – Stage1 (left) and Stage3 – Stage1 (right). The diagonal elements indicate the differences in COPD measurements acquired with identical imaging settings and serve as reference condition. Note that the ground-truth Pi10 differences were Stage2 – Stage1 = 0.10 mm and Stage3 – Stage1 = 0.32 mm.

Figure 5. Cross-section and longitudinal MAE for emphysema density.

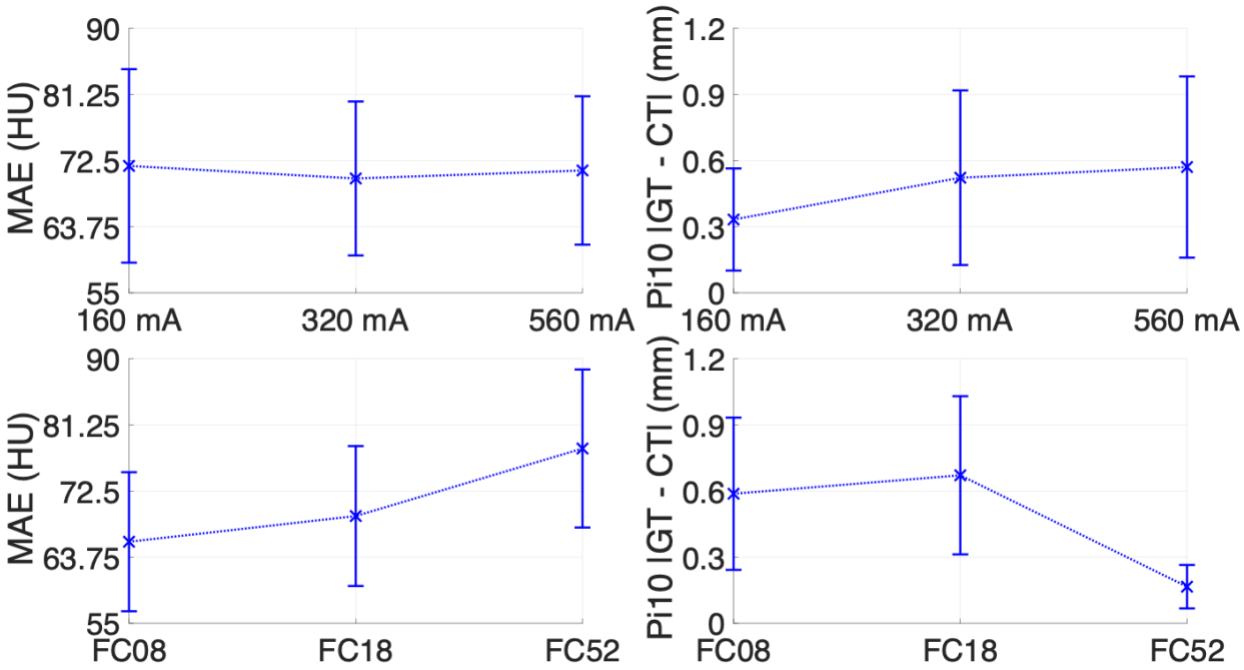

Figure 6. Cross-sectional assessment as compared to ground-truth for MAE (left column) and Pi10 (right column) measurements across three different dose levels (top row) and three kernels (bottom row).

Discussion

We successfully implemented and validated simulating a modern clinical CT scanner, incorporating its specific acquisition geometry, physics, and image reconstruction. The virtual imaging study indicated that kernel sharpness led to greater longitudinal variability in LAA-950 than dose level. MAE decreased with increasing dose; however, slightly for smooth kernels (FC08 and FC18) and significantly for the sharp kernel (FC52), highlighting the stronger influence of kernel sharpness on density measurements. When tube current was fixed, MAE increased with kernel sharpness. Similarly, under the same acquisition condition, MAE increased across the disease stages. Additionally, the sharper kernel demonstrated more accurate Pi10 measurements, emphasizing the importance of high-resolution imaging for precise bronchitis quantification.

Conclusion

Using virtual human models and a CT simulator informed with the specifications of a clinical scanner, this study evaluated the impact of imaging protocols on the accuracy of COPD biomarker measurements. In general, for both longitudinal and cross-section assessments, kernel sharpness led to more variability in the COPD measurements than the tube current did. The findings emphasize the need for standardized imaging protocols to enhance diagnostic precision and COPD patient outcomes.

Acknowledgement

The study was funded by the National Institutes of Health (P41EB028744, R01HL155293, and R01EB001838). Authors thank Canon Medical Systems for providing the information required to simulate the scanner studied in this work.

References

1. Ho FC, Sotoudeh-Paima S, Segars WP, Samei E, Abadi E. Development and Application of a Virtual Imaging Trial framework for Airway Quantifications via CT. Proc SPIE Int Soc Opt Eng. 2023; 12463.
2. Sotoudeh-Paima S, Ho FC, Nejad MG, et al. Development and Application of a Virtual Imaging Trial Framework for Longitudinal Quantification of Emphysema in CT. Proc SPIE Int Soc Opt Eng. 2024; 12925.
3. Abadi E, Segars WP, Tsui BMW, et al. Virtual clinical trials in medical imaging: a review. J Med Imaging (Bellingham). 2020; 7(4):042805.
4. Sotoudeh-Paima S, Segars WP, Ghosh D, Luo S, Samei E, Abadi E. A systematic assessment and optimization of photon-counting CT for lung density quantifications. Med Phys. 2024; 51(4):2893-904.
5. Abadi E, Jadick G, Lynch DA, Segars WP, Samei E. Emphysema Quantifications With CT Scan: Assessing the Effects of Acquisition Protocols and Imaging Parameters Using Virtual Imaging Trials. Chest. 2023; 163(5):1084-100.
6. Bhattarai M, Ho FC, Panta RK, et al. Edge-on Irradiated Silicon-Based Photon-Counting CT Vs. Energy-Integrating CT for Bronchitis Quantification: A Virtual Imaging Trial Study. AAPM 65th Annual Meeting & Exhibition: AAPM; 2023.
7. Segars WP, Bond J, Frush J, et al. Population of anatomically variable 4D XCAT adult phantoms for imaging research and optimization. Med Phys. 2013; 40(4):043701.
8. Regan EA, Hokanson JE, Murphy JR, et al. Genetic epidemiology of COPD (COPDGene) study design. COPD. 2010; 7(1):32-43.
9. Abadi E, Harrawood B, Sharma S, Kapadia A, Segars WP, Samei E. DukeSim: A Realistic, Rapid, and Scanner-Specific Simulation Framework in Computed Tomography. IEEE Trans Med Imaging. 2019; 38(6):1457-65.
10. Bhattarai M, Bache S, Abadi E, Samei E. A systematic task-based image quality assessment of photon-counting and energy integrating CT as a function of reconstruction kernel and phantom size. Med Phys. 2024; 51(2):1047-60.
11. Bhattarai M, Bache S, Abadi E, Samei E. Exploration of the pulse pileup effects in a clinical CdTe-based photon-counting computed tomography. Med Phys. 2023; 50(11):6693-703.